OsABCB14 functions in auxin transport and iron homeostasis in rice (*Oryza sativa.*L)

YanXia Xu[1,†], SaiNa Zhang[1,†], HaiPeng Guo[1], SuiKang Wang[1], LiGen Xu[1], ChuanYou Li[3], Qian Qian[4], Fan Chen[5], Markus Geisler[2], YanHua Qi[*1] and De An Jiang[*1]

[1] *State Key Laboratory of Plant Physiology and Biochemistry, College of Life Sciences, Zhejiang University, Hangzhou, China;*

[2] *Department of Biology - Plant Biology, University of Fribourg, Rue Albert-Gockel 3, CH-1700 Fribourg, Switzerland*

[3] *State Key Laboratory of Plant Genomics, National Center for Plant Gene Research, Institute of Genetics and Developmental Biology, Chinese Academy of Sciences, Beijing, China.*

[4] *State Key Laboratory of Rice Biology, China National Rice Research Institute, Chinese Academy of Agricultural Sciences, Hangzhou, China, and*

[5] *State Key Laboratory of Molecular Developmental Biology, Institute of Genetics and Developmental Biology, Chinese Academy of Sciences, Beijing, China.*

* For correspondence:

YanHua Qi,

Tel: +86 571 88981355

E-mail: qyhjp@zju.edu.cn

De An Jiang,

Tel: +86 571 88206461

Email: dajiang@zju.edu.cn

†These authors contributed equally to this work.

RUNNING TITLE: Auxin transport by rice ABCB14

SUMMARY

Members of the ATP Binding Cassette B/Multidrug-resistance/P-glycoprotein (ABCB/MDR/PGP) subfamily were shown to function primarily in auxin transport. However, none of rice ABCB transporters have been functionally characterized. Here, we describe that a knock-down of *OsABCB14* confers decreased auxin concentrations and polar auxin transport rates, conferring insensitivity to 2,4-D and IAA. OsABCB14 displays enhanced specific auxin influx activity in yeast and protoplasts prepared from rice knock-down alleles. OsABCB14 is localized at the plasma membrane pointing to an important directionality under physiological conditions. *osabcb14* mutants were surprisingly found to be insensitive to iron deficiency treatment (–Fe). Their Fe concentration is higher and up-regulation of Fe-deficiency responsive genes is lower in *osabcb14* mutants than in wild type rice, Nipponbare (NIP). Taken together, our results strongly support the role of *OsABCB14* as an

2

auxin influx transporter involved in iron homeostasis. The functional characterization of OsABCB14 provides insights in monocot auxin transport and its relationship to Fe nutrition.

KEY WORDS: OsABCB14, polar auxin transport, iron homeostasis, rice (*Oryza sativa.*L)

INTRODUCTION

Auxin regulates many aspects of plant growth and development (Woodward and Bartel, 2005; Leyser, 2006; Teale *et al.,* 2006). Auxin is thought to be synthesized in young apical tissues and then to enter basal tissues including the maturing stem and the roots by a polar transport system. The distribution of auxin and the formation of auxin gradients in the tissues are supposed to be directed by the activity of members of three families: the PIN-FORMED (PIN) family, AUXIN RESISTANT1/LIKE AUX1 (AUX1/LAX) family and ATP Binding Cassette B (ABCB) subfamily (Cho and Cho, 2012). Members of the long-looped PIN family seem to be responsible for the auxin efflux from cells (Krecek *et al.,* 2009), whereas AUX/LAX family charge the auxin influx into cells (Peret *et al.,* 2012), while the auxin transport directionality of ABCB subfamily seems to depend on cytoplasmic auxin concentration (Yang and Murphy, 2009; Abel and Theologis, 2010; Peer *et al.,* 2011).

The ABCB subfamily is the second largest ATP–binding cassette (ABC) protein subfamily and the largest full-molecule ABC transporter subfamily in plants (Rea 2007). ABCB's function in plants was first reported in the model plant *Arabidopsis thaliana* (Sidler *et al.,*

1998). For now, 5 *ABCB* genes in Arabidopsis (*AtABCB1, AtABCB4, AtABCB14, AtABCB19 and AtABCB21*) have been functionally characterized. AtABCB1 and AtABCB19 (a close homolog of AtABCB1) were demonstrated to function as auxin efflux transporters (Sidler *et al.,* 1998; Noh *et al.,* 2001; Geisler *et al.,* 2003; Geisler *et al.,* 2005; Cho *et al.,* 2007; Wang *et al.,* 2013). AtABCB4 and AtABCB21（a close homolog of AtABCB4）were reported to have facultative auxin transport function, depending on auxin concentrations – auxin uptake activity at low auxin concentrations and invert to export activity at high auxin concentrations (Terasaka *et al.,* 2005; Yang and Murphy, 2009; Kamimoto *et al.,* 2012; Kubes *et al.,* 2012). Additionally, AtABCB14 is a malate uptake transporter and plays an essential role under stress conditions (Lee *et al*., 2008). Studies of ABCBs in other species showed that ABCBs also able to transport secondary metabolites (Shitan *et al*., 2003) and to regulate aluminum tolerance and calcium homeostasis (Sasaki *et al*., 2002).

In Arabidopsis, evidences have been provided that the members of PIN and ABCB protein families regulate auxin transport coordinately and independently (Noh *et al*., 2003; Bandyopadhyay *et al*., 2007; Blakeslee *et al*., 2007; Mravec *et al*., 2008; Titapiwatanakun *et al*., 2009). Some studies also focused on the interaction between ABCBs and the immunophilin-like FKBP42, TWISTED DWARF1 (TWD1), and the protein phosphorylation of ABCBs. AtABCB1 was reported to be substrate of PINOID (PID), an AGC kinase. TWD1 interacts with PID, and directs phosphorylation of ABCB1 in a regulatory linker domain that alters ABCB1-mediated auxin transport activity (Geisler *et al.,* 2003; Geisler *et al.,* 2004; Bouchard *et al.,* 2006; Bailly *et al.,* 2008; Henrichs *et al.,* 2012). AtABCB19 also can be

phosphorylated by PHOTOTROPIN 1 (phot1), a plasma membrane serine-threonine protein kinase involved in blue-light responses, to inhibit its efflux activity (Christie *et al.,* 2011). All these above results were mainly established using dicotyledonous Arabidopsis as a model system, but the role of ABCBs is unclear in monocotyledons.

Several studies indicate a close interrelationship between auxin and iron ion homeostasis: auxin has been already reported since the 80s to be implicated in iron deficiency-induced adaptive responses (Landsberg, 1981). Sunflower roots, were shown to own higher levels of auxin under Fe-deficient condition than Fe-sufficient (Römheld and Marschner, 1986). Reductions of auxin transport or auxin sensitivity all inhibited formation of root hair in response to Fe-deficiency (Schikora and Schmidt, 2001). Further, the influence of plant hormones on Fe uptake by strategy I plants was summarized in Romera *et al.* (2007). Based on reports from recent years, Fe deficiency can trigger an over-accumulation of indole-3-acetic acid (IAA) and Arabidopsis auxin transporter *aux1-7* mutant plants exhibit reduced ferric chelate reductase activity under low Fe (Chen *et al*., 2010). Thus, the auxin transporter AtAUX1 is thought to mainly direct the root-ward auxin stream into lateral roots to integrate local Fe nutritional status (Giehl *et al.,* 2012). In *Malus xiaojinensis,* it is also indicated that iron deficiency-induced physiological responses are mediated by systemic auxin signaling (Wu *et al*., 2012). We also reported that auxin response factor, OsARF12, regulates root elongation and affects in iron homeostasis in rice (Qi *et al*., 2012). However, the molecular mechanism of auxin in the regulation of iron deficiency responses still maintains unclear in monocot, needs to be systematically investigated further.

It is important to note that, although rice is an important food crop, there are no reports on its ABCBs. To test whether ABCB also play an important role in rice, we investigated the behavior of *OsABCB14* gene in rice. OsABCB14 is shown to function in cellular auxin uptake and iron homeostasis in rice.

RESULTS:

Identification of *osabcb14* mutants and complemented transgenic lines

We obtained two TOS17 insertional lines in the *OsABCB14* gene from the Rice Genome Resource Center in Japan. Using PCR analysis and sequencing, we confirmed that TOS17 had been inserted into the 8th exon of the *OsABCB14* gene at *osabcb14-1*, and 7th intron of *OsABCB14* in *osabcb14-2*, respectively (Figure 1a). Both mutant lines are homozygous (Figure 1b). In addition, we overexpressed *OsABCB14* in *osabcb14-1* and *osabcb14-2* under the control of a CaMV35S promoter to create the complemented transgenic lines. Reverse transcriptase real-time PCR (RT-PCR) and quantitative real-time PCR (qRT-PCR) using three pair of primers (located around the insertion sites, 5' regions and 3' regions, respectively) showed that the expression of *OsABCB14* was ~5 folds lower in both mutant lines and ~5 folds higher in both complementation lines (*osabcb14-1*C and *osabcb14-2*C) than that in wild type (NIP) (Figure 1c,d).

AtABCB1and AtABCB19, the two closest relatives of OsABCB14 (Shen *et al*., 2010), were reported to transport auxin. This led us to ask whether OsABCB14 was involved in auxin

transcript. We first investigated the phenotypes of shoots and primary roots (PRs) of NIP, *osabcb14* mutants and *osabcb14*C. The shoot and PR lengths in NIP for 7d seedling were only slightly shorter than those of *osabcb14-1* and *osabcb14-2* under normal conditions (CK) (Figure 1e), while significantly shorter than those of *osabcb14-1* and *osabcb14-2* under 0.01μM 2,4-D treatment (Figure 1f). Similar results were obtained when grown in the nutritional solution containing 10μM IAA (Figure 1g). However, there was no difference between NIP and *osabcb14* mutants under treatment of 0.001~1μM NAA (Figure S1). We further performed a dose-response assay to confirm the effect of 2,4-D, IAA and NAA in more details. High concentration of all the three auxins inhibited the shoot and PR growth, but more prominent in NIP than *osabcb14* mutants under 2,4-D treatment at a concentration of $>10^{-8}$ mol l^{-1} (Figure 1h,i) and IAA treatment at a concentration of $>10^{-7}$ mol l^{-1} (Figure 1j,k), while no significant difference under NAA treatment (Figure S1). All these phenotypes in *osabcb14* mutants could be reverted by transgenic lines *osabcb14*C (Figure 1e-k). These results confirmed that *osabcb14* mutants are insensitive to 2,4-D and IAA, but not responsive to NAA. These observations were similar to the previous studies on AUX1 (Delbarre *et al.,* 1996; Yang *et al.*, 2006), suggesting that OsABCB14 is required for auxin transport in either shoot or root.

Expression pattern and subcellular localization of OsABCB14

To explore the *in vivo* function of *OsABCB14*, we first analyzed the expression pattern of *OsABCB14*. The expression pattern of *OsABCB14* was analyzed in different organs and growth stages using qRT-PCR. The results showed that *OsABCB14* expression is constitutive

in various organs. At all growth stages observed, *OsABCB14* was ubiquitously expressed in all plant organs, including the root, stem, leaf, node, root-stem transition region, filling seed, panicle and flower (Figure 2a). Spatial expression analysis showed that the expression of *OsABCB14* was higher in root tips than in the basal root zones (Figure 2b). GUS staining revealed that *OsABCB14* is expressed in the root tip and stele of the PR and leaves. Cross section of leaf sheath showed that *OsABCB14* is expressed in the vascular (Figure 2c-f). *OsABCB14* is also strongly expressed in node, internode, root-stem transition region and flowers (Figure 2g-j).

To investigate the relationship between *OsABCB14* and phytohormones, including auxin, the expression of *OsABCB14* under various phytohormones and polar auxin transport inhibitors treatment was analyzed by qRT-PCR. As shown in Figure 2k and Figure S2a, the expression of *OsABCB14* was greatly induced by 2,4-D, IAA, 6-BA, ABA, SA or NOA treatment. However, the expression of *OsABCB14* was only slightly up-regulated under NAA, GA$_3$ and NPA treatment. Furthermore, when treated by 1μm 2,4-D or 10μm IAA, the expression of *OsABCB14* was strongest induced after 12h (Figure 2l,m; Figure S2b,c).

To determine the subcellular localization of the OsABCB14 protein, *OsABCB14* was cloned into pH7FWG2 and that like fused with the enhanced green fluorescent protein (EGFP). Transient expression of OsABCB14 in the epidermis cells of *N. benthamiana* leaves and onion epidermis indicating that OsABCB14 was localized at the plasma membrane (Figure 3a-c).

osabcb14-1 and _osabcb14-2_ mutants own reduced auxin concentrations

Loss-of-function mutation of AtAUX1, which is an auxin influx transporter, resulted in reduced auxin concentration and auxin transport (Yu and Wen 2013). In addition, the loss-of-mutations of AtABCB19 identified as auxin efflux transporters also led to reduced auxin concentration and auxin transport (Noh _et al.,_ 2001). To determine whether the knockdown of OsABCB14 also alters auxin concentration and auxin transport in rice, we measured the auxin concentration and polar auxin transport in NIP and _osabcb14_ mutants. The results showed that the auxin concentrations of _osabcb14-1_ and _osabcb14-2_ in both shoot and root were significantly lower than in NIP (Figure 4a,b). The staining of _DR5:GUS_, a biological marker to study the native auxin distribution, was observed in NIP and _osabcb14_ mutants (Figure 4c,d), and the results coincided with the above measurements. In addition, examination of the transcription of well-characterized auxin-responsive genes in _osabcb14_ mutants showed that mRNA levels of _OsIAA3_, _OsIAA9_, _OsIAA23_ and _OsSAUR39_ were down-regulated in _osabcb14_ mutants (Figure 4e,f), which is hence consistent with the reduced auxin sensitivity and auxin concentration in _osabcb14_ mutants.

Auxin transport activity in yeast and _osabcb14_ mutants

Reduced auxin sensitivities and auxin levels prompted us to quantify auxin transport capacities of OsABCB14. First, we functionally expressed OsABCB14 in the baker's yeast. Yeast expressing _OsABCB14_ accumulated 3-times more IAA than the vector control, indicating an auxin uptake activity for OsABCB14 (Figure 5a). Auxin uptake by OsABCB14 was specific as the diffusion control benzoic acid (BA) was not transported differently to the

9

vector control. Next, we quantified auxin loading (= influx) into rice protoplasts not yet shown before. Both *osabcb14* alleles revealed significantly reduced auxin loading, pointing again to an auxin import activity of OsABCB14 (Figure 5b). In order to test the facultative efflux capacity of OsABCB14 reported for Arabidopsis orthologs AtABCB4 and AtABCB21 (Terasaka *et al.,* 2005; Yang and Murphy, 2009; Kamimoto *et al.,* 2012; Kubes *et al.,* 2012), we quantified also IAA efflux after loading of protoplasts. Interestingly, both *osabcb14* alleles revealed significantly enhanced IAA export indicating again a preferred import directionality for OsABCB14, that when absent reduces efflux most probably by lack of re-import of effluxed IAA (Figure 5c). In analogy to auxin treatments, no import of NAA by OsABCB14 was found known to be not dependent on auxin uptake systems as it can freely diffuse into cells (Delbarre *et al.,* 1996; Yang *et al.*, 2006). Finally, acropetal auxin transport of *osabcb14-1* and *osabcb14-2* roots was found to be decreased $\sim$ 59％ and 63％, respectively, in comparison to NIP (Figure 5d), while basipetal auxin transport was not different from NIP (Figure 5e). This suggests in summary that OsABCB14 functions as an auxin importer involved in acropetal transport but not basipetal transport of auxin.

osabcb14 mutants are insensitive to Fe deficiency and Os*ABCB14* was involved in iron homeostasis

TaABCB1 was reported to be involved in aluminum tolerance and calcium homeostasis in wheat (Sasaki *et al.*, 2002). To test whether OsABCB14 is also functionally related to ion homeostasis, we measured the metal ion concentrations in the seeds, shoots and roots of NIP

and *osabcb14* mutants. As shown in Figure 6a, the Fe concentrations in the seeds, shoots and roots of the two *osabcb14* mutant lines were all significantly higher (56％ higher in *osabcb14-1* and 43％ higher in *osabcb14-2* for seeds; 51％ higher in *osabcb14-1* and 38％ higher in *osabcb14-2* for shoots; 35％ higher in *osabcb14-1* and 40％ higher in *osabcb14-2* for roots) than that in NIP. The concentrations of the other metals, such as Mn, Cu, Zn, and Mg were also enhanced in the *osabcb14* mutants than in NIP (Figure S3). These results suggested that Os*ABCB14* might be involved in ion homeostasis.

To understand the relationship between OsABCB14 and Fe homeostasis, we further investigated the phenotypes of *osabcb14* mutants under iron-deficient nutrient solution (–Fe). *osabcb14* mutants displayed significantly longer shoots and roots than NIP under –Fe conditions, but only slightly longer roots than NIP and normal shoot length under CK (Figure 6b-d). The chlorophyll concentration of *osabcb14* mutants was significantly higher (161％ in *osabcb14-1* and 183％ in *osabcb14-2*) than that of NIP under –Fe (Figure 6e). In addition, the differences of Fe concentration between NIP and *osabcb14* mutants were more obvious under –Fe treatment (65％ and 40％ higher in shoots and roots of *osabcb14-1* , 40％ and 43％ higher in shoots and roots of *osabcb14-2*) (Figure 6f-g) compared to CK (Figure 6a). These results suggest that *osabcb14* mutants are insensitive to –Fe.

The enhanced Fe concentration in both shoots and roots of *osabcb14* mutants under CK and –Fe may have been due to enhanced Fe concentration in the seeds or the impaired Fe uptake

or homeostasis or both of them. To evaluate the effect of *OsABCB14* disruption on the rice Fe

uptake and signaling system, we analyzed the expression level of Fe-deficiency responsive

genes *IRT1* (Fe-regulated transporter 1), *IRT2*, *IRO2* (Fe-responsive operator 2), *YSL15*

(yellow-stripe like 15), *NAAT1* (nicotianamine aminotransferase 1), *NRAMP2* (natural

resistance-associated macrophage protein 2), *NAS1* (nicotianamine synthase) and *NAS2*. The

results showed that the expression of all these genes was up-regulated in *osabcb14* mutants

(Figure 7a, S4a). These genes were reported to be up-regulated under –Fe (Jia *et al.,* 2011; Qi

et al., 2012). Consisted with that, qRT-PCR analysis here showed that all these genes were

induced in NIP and *osabcb14* mutants under –Fe, but the induced folds in *osabcb14* mutants

were significantly lower than that in NIP (Figure 7b; Figure S4b). This result closely

coincided with the observations above – *osabcb14* mutants are insensitive to Fe deficiency.

DISCUSSION

In the rice genome, 22 *ABCB* genes have been identified (Shen *et al.*, 2010), but not one of

them has been functionally characterized. Here, we report the biological function of

OsABCB14 in auxin uptake and iron homeostasis in rice.

Evidence presented in this and other articles demonstrates that many ABCB family members

play critical roles in auxin-dependent development processes. For example, research on

AtABCB1 and AtABCB19, whose overexpression and disruption led to de-regulation of root

elongation, gravitropism and phototropism (Noh *et al.*, 2003; Lewis *et al.*, 2007; Wu *et al.*,

2007), suggests that they are involved in auxin-dependent programs. Several studies also

supported the role for AtABCB4 in auxin-mediated developmental process, mainly in root elongation (Santelia *et al*., 2005; Terasaka *et al.*, 2005). OsABCB14 as the closest rice ortholog of AtABCB1 and AtABCB19, conferred altered sensitivity to high concentrations of 2,4-D and IAA (Figure 1e-k), suggesting its involvement in auxin-mediated program.

Reduced responses of *osabcb14-1* and *osabcb14-2* to 2,4-D and IAA are similar to the previous studies on AtAUX1 (Yang *et al.,* 2006). 2,4-D as a synthetic auxin that is transported into plant cells predominantly by a carrier (Delbarre *et al.*, 1996; Yamamoto and Yamamoto, 1998), can serve very well to assess the activity of auxin uptake carriers (Hoyerova *et al*., 2008). A defect in the auxin uptake carrier is expected to lead to a decreased sensitivity to high concentrations of 2,4-D and both *osabcb14* mutants exhibited that phenotype, suggesting that *OsABCB14* may play an important role in the influx phase of polar auxin transport. These data are supported by the finding that *osabcb14* shows an unaltered sensitivity to the synthetic auxin, NAA (Figure S1), known to be independent of an uptake system, such as AUX1 (Delbarre *et al.*, 1996; Yamamoto and Yamamoto, 1998) or ABCB4-like ABCBs (Kamimoto *et al.,* 2012).

Results of IAA transport analysis from yeast and leaf protoplasts prepared from knock-down rice mutants alleles verify that OsABCB14 functions as an auxin transporter and are in complete accordance with an uptake or import directionality (Figure 5). This finding is slightly surprising because OsABCB14 clusters closer to Arabidopsis ABCB19 (and ABCB1) than to ABCB4/ABCB21 that was characterized as exporter and facultative im/exporters,

13

respectively. However, our data (especially efflux experiments from rice protoplasts; Figure 5c) indicate that OsABCB14 functions under tested conditions primarily as importer. Therefore these data also suggest that transport directionalities cannot simply be deduced by phylogenetic analyses or that transport directionalities are achieved differently in monocots and dicots.

Acropetal auxin transport of both *osabcb14* mutant roots was significantly lower than in NIP, suggesting that OsABCB14 functions in acropetal (root-ward) polar auxin transport. As a result knock-down roots of *OsABCB14* displayed reduced auxin concentrations and DR5:GUS activity (Figure 4a-d), most probably caused by reduced auxin delivery from the shoot. Interestingly, also shoot IAA levels were strongly reduced in both mutant alleles suggesting altered shoot transport. However, we failed to quantify shoot transport in *osabcb14* alleles reliably because measurements of shoot transport are still a technical challenge in rice. However, we speculate that like in roots probably also acropetal (= shoot-ward) auxin transport might be reduced in *osabcb14* shoots. Reduced acropetal PAT capacities and auxin levels in the mutant, however, are also in agreement with described roles for AUX1 in acropetal auxin transport in the Arabidopsis root (Yu and Wen 2013). Therefore, this result also adds to the growing evidences supporting a major role of ABCBs in polar auxin transport.

In summary, our study provides convincing evidence for OsABCB14 as a plasma membrane auxin influx transporter (Figure 1, 3, 4, 5). However, we surprisingly found that OsABCB14

is also involved in ion homeostasis. Fe, Mn, Cu, Zn, Mg and Ca are important nutrient element for plants growth and development. Fe concentration of *osabcb14* mutants in shoots, roots and seeds were significantly enhanced (Figure 6a) and the expression level of Fe-deficiency responsive genes was significantly up-regulated in *osabcb14* mutants (Figure 7a; Figure S4a). Thus, increased Fe concentrations in shoot and root of *osabcb14* mutants (fourteen-day old) due to not only the higher Fe concentrations in seeds but also the up-regulated expression level of Fe-deficiency responsive genes. In addition, *osabcb14* mutants displayed insensitive phenotype and less reduced gene expression level to –Fe (Figure 6b-e, 7b; Figure S4b) and increased Mn, Cu, Zn and Mg concentration (Figure S3). Together, these results suggest that disruption of *OsABCB14* could affect negatively iron and homeostasis of other metal ions. Seeds of *osabcb14* mutants have higher Fe concentration (56％ higher in *osabcb14-1* and 43％ higher in *osabcb14-2*) (Figure 6a), indicating that *osabcb14* mutants maybe can be used for creating iron-enriched crops. In the dicot Arabidosis, auxin importer AUX1 was also shown to be involved in Fe deficiency and the enhanced elongation of lateral roots in response to local Fe was demonstrated to depend on AUX1 action (Chen *et al*., 2010, Giehl *et al.,* 2012). Thus, OsABCB14 may affect ion transport though the regulation of down-stream ion transporters. A systematic transcriptome analysis of *osabcb14* mutants grown under CK and –Fe will elucidate (out) related genes in Fe and auxin signaling systems.

EXPERIMENTAL PROCEDURES:

Plant materials and growth conditions

Rice plants (*Oryza sativa* L.) were grown in normal culture solution containing 1.425 mM NH_4NO_3, 0.323 mM NaH_2PO_4, 0.513 mM K_2SO_4, 0.998 mM $CaCl_2$, 1.643 mM $MgSO_4$, 0.25 mM $NaSiO_3$, 0.009 mM $MnCl_2$, 0.019 µM H_3BO_3, 0.152 µM $ZnSO_4$, 0.155 µM $CuSO_4$, 0.075 µM $(NH_4)_6Mo_7O_{24}$ and 0.125 mM EDTA-Fe (II) (Yoshida *et al.,* 1976) without (CK) or with treatments, pH=5.2~5.5. Rice plants were grown in growth chambers with 60-70％ humidity and a light/dark cycle of 12/12 h at 30/24°C. For transient expression, *Nicotiana benthamiana* plants were grown in vermiculite containing Murashige and Skoog salt nutritional liquid in a growth chamber with 60-70％ humidity and a light/dark cycle of 12/12 h at 25/18°C.

Identification of the *osabcb* mutants

Two TOS17 insertion lines for *OsABCB14*, *osabcb14-1* (NF6030) and *osabcb14-2* (NG3129), were obtained from the Rice Genome Resource Center in Japan. The homozygous lines was screened by PCR, using primer TOS17-tail6 to confirm the integration of TOS17 in two mutant lines and gene-specific primers ABCB14-1U/L and ABCB14-2U/L to identify wild-type (NIP)-bound *OsABCB14*. The PCR insertion products were ligated with pMD19-T Simple Vector (TaKaRa, Japan) and transformed into *Escherichia coli* DH5α, and the flanking sequences of the TOS17 insertion site were sequenced by Invitrogen (Shanghai, China). To confirm that the transcription level of the *OsABCB14* gene in the NIP and two TOS17 homozygous lines, RT-PCR was performed using three pairs of primers, RTABCB14U1/L1, RTABCB14U2/L2 and RTABCB14U3/L3. qRT-PCR was performed

using another three pairs of primers, qRTABCB14U1/L1, qRTABCB14U2/L2 and qRTABCB14U3/L3. Primer sequences for the PCR and RT-PCR are listed in Table S1.

Vector construction

The *OsABCB14* (Os04g38570) coding region was amplified from the full-length cDNA (AK103526) using primers ABCB14-OU/L (Table S1) for cloning into pH7FGW2 to create ABCB14: EGFP fusion construct according to the manufacturer's instructions (Invitrogen). The final construct *35S:ABCB14-EGFP* was transiently expressed in the leaves of *N. benthamiana* plants and onion as previously described (Qi *et al*., 2012). After 2d, the fluorescence was visualized under the confocal microscopy (Zeiss Leica TCS SP5; Mannheim, Germany) as described (Guo *et al*., 2003). These constructs were also introduced into *Agrobacterium tumefaciens* strain EHA105 using electroporation and transferred into *osabcb14-1* and *osabcb14-2* using callus infection method (Hiei *et al*., 1994) for complementation constructs. To analysis the transcription level of the *OsABCB14* gene in the complementation lines, the primers RTABCB14U1/L1 and qRTABCB14U1/L1 listed in Table S1 were used.

To construct *ProOsABCB14:GUS*, a 2.1kb promoter region of the *OsABCB14* gene was amplified by PCR using primers ABCB14-proU/L (listed in TableS1) for cloning into *Sal*I-*Kpn*I site of pBI101.3-GUS-plus. The final construct *ProOsABCB14:GUS* was introduced into *Agrobacterium tumefaciens* strain EHA105 using electroporation and transferred into NIP using callus infection method (Hiei *et al*., 1994).

Analysis of IAA concentrations and transport

Free IAA concentrations in seedling tissues were performed as described previously (Shen *et al*., 2013). Briefly, 20 mg of fresh shoots or roots of seven-day seedlings grown on normal nutrient solution were washed by sterile deionized water several times. The samples were then ground into fine powder in liquid nitrogen and dissolved in 50 mM KH2PO4–NaOH with 0.02% (w/v) ascorbic acid, then 250 pg of ^{13}C-IAA were added to each sample solution. Free IAA concentrations were measured by gas chromatography-selected reaction monitoring mass spectrometry. The *DR5:GUS* construct was transformed into NIP and *osabcb14* mutants to detect auxin distribution in T2 generation. For staining of *DR5:GUS* seedlings, 100mM sodium phosphate buffer (PH7.0) containing 0.1％ v/v Triton X-100 and 2mM X-Gluc was used. Tissues were vacuum infiltrated for 15 min with staining solution and incubated for 30 min at 37°C before being observed using a Zeiss Leica TCS SP5 (Mannheim, Germany). Analyses of polar ^{3}H-IAA transport were performed according to Qi *et al.,* (2008).

Yeast auxin loading experiments were performed as in Kamimoto *et al* (2012). In brief, JK93da transformants were grown to OD600 = 1, washed and incubated at 30°C with 1 ml/ml 5-[^{3}H]IAA (specific activity 7.4×10^{11} Bq/mmol, American Radiolabeled Chemicals) and [^{3}H]BA (9.3×10^{11} Bq/mmol, American Radiolabeled 60 Chemicals) in SD media (pH 5.5). Aliquots of 1ml were filtered twice with cold water after 0 and 10 minutes, respectively, and the retained radioactivity was quantified by scintillation counting. Rice protoplasts were prepared as described in Zhang *et al* (2011) with the exception that leaf digests were performed over-night. Transport assays were performed as described in Henrichs *et al* (2012).

In brief, intact protoplasts were loaded by incubation with 1 ul/ml [³H]IAA (specific activity 7.4×10^{11} Bq/mmol, American Radiolabeled Chemicals) and 4-[³H]NAA (9.3×10^{11} Bq/mmol, American Radiolabeled Chemicals) in the presence of 100 nM IAA on ice. Import was started by incubation at 25°C and halted after 10 minutes by silicon oil centrifugation. For export assays, loading was performed for 10 min on ice, allowing equal loading and external radioactivity was removed by Percoll gradient centrifugation. Imported/exported radioactivity was determined by scintillation counting of the protoplast interfaces/supernatants, respectively, and is presented as the relative export/import of the initial export/uptake (export/import prior to temperature incubation).

Metal ion concentrations assay

Rice seedling grown in hydroponics to two-weeks old and peeled rice seeds were analyzed to determine their metal ion concentrations with inductively coupled plasma mass spectrometry (Agilent 7500ce; Agilent Technologies, Palo Alto, CA, USA) as previously described (Jia *et al.,* 2011). Five biological replicates were performed for each sample.

Measurement of chlorophyll concentrations

The leaves of NIP and *osabcb14* mutants grown in CK and –Fe for two weeks were collected and weighed for their fresh weight. Chlorophyll was extracted with ethanol for 24h and the concentration was assayed based on the absorbance of the extract at 645, 652 and 663 nm (Wintermans and De Mots, 1965).

RT-PCR and qRT-PCR

The methods of total RNA extraction, reverse transcription, and RT-PCR were as found in a previous report (Qi *et al.*, 2012). Primer sequences for auxin-responsive genes and Fe-deficiency responsive genes are listed in Table S2 and Table S3, respectively.

SUPPORTING INFORMATION

Figure S1. Phenotype of *osabcb14* mutants and complemented transgenic lines under NAA treatment.

Figure S2. Expression of *OsABCB14* in roots responded to various treatments.

Figure S3. Mn, Cu, Zn, Mg and Ca concentrations (µg/g) in leaf and root of *osabcb14*

mutants.

Figure S4. Relative expression of genes related to Fe uptake and transport in roots of NIP and *osabcb14* mutants.

Table S1. Primer sequences of *OsABCB14*.

Table S2. Primer sequences for auxin-responsive genes.

Table S3. Primer sequences for Fe-deficiency responsive genes.

REFERENCES

Abel, S., and Theologis, A. (2010) The odyssey of auxin. Cold Spring Harb Perspect Biol. **2**, a004572.

Bailly, A., Sovero, V., Vincenzetti, V., Santelia, D., Bartnik, D., Koenig, B.W., Mancuso, S., Martinoia, E., and Geisler, M. (2008) Modulation of P-glycoproteins by auxin transport inhibitors is mediated by interaction with immunophilins. *J. Biol. Chem.* **28**, 21817–21826.

Bandyopadhyay, A., Blakeslee, J.J., Lee, O.R., Mravec, J., Sauer, M., Titapiwatanakun, B., Makam, S.N., Bouchard, R., Geisler, M., Martinoia, E., Friml, J., Peer, W.A. and Murphy, A.S. (2007) Interactions of PIN and ABCB auxin transport mechanisms. *Biochem. Soc. Trans.* **35**, 137–141.

Blakeslee, J.J., Bandyopadhyay, A., Lee, O.R., Mravec, J., Titapiwatanakun, B., Sauer,

M., Makam, S.N., Cheng, Y., Bouchard, R., Adamec, J., Geisler, M., Nagashima, A., Sakai, T., Martinoia, E., Friml, J., Peer, W.A. and Murphy, A.S. (2007) Interactions among PINFORMED and P-glycoprotein auxin transporters in *Arabidopsis thaliana*. *Plant Cell,* **19**, 131–147.

Bouchard, R., Bailly, A., Blakeslee, J.J., Oehring, S.C., Vincenzetti, V., Lee, O.R., Paponov, I., Palme, K., Mancuso, S., Murphy, A.S., Schulz, B., and Geisler, M. (2006) Immunophilin-like TWISTED DWARF1 modulates auxin efflux activities of Arabidopsis P-glycoproteins. *J. Biol. Chem.* **281**, 30603–30612.

Chen, W.W., Yang, J.L., Qin, C., Jin, C.W., Mo, J.H., Ye, T. and Zheng, S.J. (2010) Nitric oxide acts downstream of auxin to trigger root ferric-chelate reductase activity in response to iron deficiency in Arabidopsis. *Plant Physiol.* **154**, 810–819.

Cho, M. and Cho, H.T. (2012) The function of ABCB transporters in auxin transport. *Plant Signal Behav.* 8, pii: e22990.

Cho, M., Lee, S.H. and Cho, H.T. (2007) P-glycoprotein4 displays auxin efflux transporter-like action in Arabidopsis root hair cells and tobacco cells. *Plant Cell,* **19**, 3930–3943.

Christie, J.M., Yang, H., Richter, G.L., Sullivan, S., Thomson, C.E. Lin, J., Titapiwatanakun, B., Ennis, M., Kaiserli, E., Lee, O.R., Adamec, J., Peer, W.A., and Murphy, A.S. (2011) phot1 inhibition of ABCB19 primes lateral auxin fluxes in the shoot apex required for phototropism. *PLoS Biol.* **9**:e1001076.

Delbarre, A., Muller, P., Imhoff, V., and Guern, J. (1996) Comparison of mechanisms controlling uptake and accumulation of 2,4-dichlorophenoxy acetic acid,

naphthalene-1-acetic acid, and indole-3-acetic acid in suspension-cultured tobacco cells. *Planta,* **198**, 532-541.

Geisler, M., Blakeslee, J.J., Bouchard, R., Lee, O.R., Vincenzetti, V., Bandyopadhyay, A., Titapiwatanakun, B., Peer, W.A., Bailly, A., Richards, E.L., Ejendal, K.F., Smith, A.P., Baroux, C., Grossniklaus, U., Müller, A., Hrycyna, C.A., Dudler, R., Murphy, A.S. and Martinoia, E. (2005) Cellular efflux of auxin catalyzed by the Arabidopsis MDR/ABCB transporter AtABCB1. *Plant J.* **44**, 179–194.

Geisler, M., Girin, M., Brandt, S., Vincenzetti, V., Plaza, S., Paris, N., Kobae, Y., Maeshima, M., Billion, K., Kolukisaoglu, U.H., Schulz, B., and Martinoia, E. (2004) Arabidopsis immunophilin-like TWD1 functionally interacts with vacuolar ABC transporters. *Mol. Biol. Cell,* **15**, 3393–3405.

Geisler, M., Kolukisaoglu, H.U., Bouchard, R., Billion, K., Berger, J., Saal, B., Frangne, N., Koncz-Kalman, Z., Koncz, C., Dudler, R., Blakeslee, J.J., Murphy, A.S., Martinoia, E. and Schulz, B. (2003) TWISTED DWARF1, a unique plasma membrane-anchored immunophilin-like protein, interacts with Arabidopsis multidrug resistance-like transporters AtABCB1 and AtABCB19. *Mol. Biol. Cell,* **14**, 4238-4249.

Giehl, R.F., Lima, J.E. and von Wirén, N. (2012) Localized iron supply triggers lateral root elongation in Arabidopsis by altering the AUX1-mediated auxin distribution. *Plant Cell*, **24**, 33-49.

Guo, F., Young, J. and Crawford, N. (2003) The nitrate transporter AtNRT1.1 (CHL1) functions in stomatal opening and contributes to drought susceptibility in Arabidopsis. *Plant Cell,* **15**, 107–117.

Henrichs, S., Wang, B., Fukao, Y., Zhu, J., Charrier, L., Bailly, A., Oehring, S.C., Linnert, M., Weiwad, M., Endler, A., Nanni, P., Pollmann, S., Mancuso, S., Schulz, A., and Geisler, M. (2012) Regulation of ABCB1/ABCB1-catalysed auxin transport by linker phosphorylation. *EMBO J*. doi: 10.1038.

Hiei, Y., Ohta, S., Komari, T. and Kumashiro, T. (1994) Efficient transformation of rice (Oryza sativa L.) mediated by Agrobacterium and sequence analysis of the boundaries of the T-DNA. *Plant J.* **6**, 271–282.

Hoyerová, K., Perry, L., Hand, P., Lanková, M., Kocábek, T., May, S., Kottová, J., Paces, J., Napier, R. and Zazímalová, E. (2008) Functional characterization of PaLAX1, a putative auxin permease, in heterologous plant systems. *Plant Physiol.* **146**, 1128-1141.

Jia, L., Wu, Z., Hao, X., Carrie, C., Zheng, L., Whelan, J., Wu, Y., Wang, S., Wu, P., and Mao, C. (2011) Identification of a novel mitochondrial protein, short postembryonic roots 1 (SPR1), involved in root development and iron homeostasis in Oryza sativa. *New Phytol.* **189**, 843–855.

Kamimoto, Y., Terasaka, K., Hamamoto, M., Takanashi, K., Fukuda, S., Shitan, N., Sugiyama, A., Suzuki, H., Shibata, D., Wang, B., Pollmann, S., Geisler, M. and Yazaki, K. (2012) Arabidopsis ABCB21 is a facultative auxin importer/exporter regulated by cytoplasmic auxin concentration. *Plant Cell Physiol.* **53**, 2090-2100.

Krecek, P., Skupa, P., Libus, J., Naramoto, S., Tejos, R., Friml, J. and Zazímalová, E. (2009) The PIN-FORMED (PIN) protein family of auxin transporters. *Genome Biol.* **10**, 249.

Kubeš, M., Yang, H., Richter, G.L., Cheng, Y., Młodzińska, E., Wang, X., Blakeslee, J.J., Carraro, N., Petrášek, J., Zažímalová, E., Hoyerová, K., Peer, W.A. and Murphy, A.S. (2012) The Arabidopsis concentration-dependent influx/efflux transporter ABCB4 regulates cellular auxin levels in the root epidermis. *Plant J.* **69**, 640-654.

Landsberg, E.C. (1981) Fe stress induced transfer cell formation: regulated by auxin? *Plant Physiol.* **67**, 563.

Lee, M., Choi, Y., Burla, B., Kim, Y.Y., Jeon, B., Maeshima, M., Yoo, J.Y., Martinoia, E. and Lee, Y. (2008) The ABC transporter AtABCB14 is a malate importer and modulates stomatal response to CO_2. *Nat. Cell Biol.* **10**, 1217–1223.

Lewis, D.R., Miller, N.D., Splitt, B.L., Wu, G. and Spalding, E.P. (2007) Separating the roles of acropetal and basipetal auxin transport on gravitropism with mutations in two Arabidopsis multidrug resistance-like ABC transporter genes. *Plant Cell,* **19**, 1838–1850.

Leyser, O. (2006) Dynamic integration of auxin transport and signaling. *Curr. Biol.* **16**, R424–R433.

Mravec, J., Kubes, M., Bielach, A., Gaykova, V., Petrásek, J., Skůpa, P., Chand, S., Benková, E., Zazímalová, E. and Friml, J. (2008) Interaction of PIN and ABCB transport mechanisms in auxin distribution-dependent development. *Development,* **135**, 3345–3354.

Nelson, B.K., Cai, X. and Nebenführ, A. (2007) A multicolored set of in vivo organelle markers for co-localization studies in Arabidopsis and other plants.

Plant J. **51**, 1126-1136.

Noh, B., Bandyopadhyay, A., Peer, W.A., Spalding, E.P. and Murphy, A.S. (2003)

Enhanced gravi- and phototropism in plant mdr mutants mislocalizing the auxin efflux protein PIN1. *Nature,* **423**, 999–1002.

Noh, B., Murphy, A.S. and Spalding, E.P. (2001) Multidrug resistance-like genes of Arabidopsis required for auxin transport and auxin-mediated development. *Plant Cell*, **13**, 2441–2454.

Peer, W.A., Blakeslee, J.J., Yang, H., and Murphy, A.S. (2011) Seven things we think we know about auxin transport. *Mol. Plant*, **4**, 487-504.

Péret, B., Swarup, K., Ferguson, A., Seth, M., Yang, Y., Dhondt, S., James, N., Casimiro, I., Perry, P., Syed, A., Yang, H., Reemmer, J., Venison, E., Howells, C., Perez-Amador, M.A., Yun, J., Alonso, J., Beemster, G.T., Laplaze, L., Murphy, A., Bennett, M.J., Nielsen, E. and Swarup, R. (2012) AUX/LAX genes encode a family of auxin influx transporters that perform distinct functions during Arabidopsis development. *Plant Cell,* **24**, 2874-2885.

Qi, J., Qian, Q., Bu, Q., Li, S., Chen, Q., Sun, J., Liang, W., Zhou, Y., Chu, C., Li, X., Ren, F., Palme, K., Zhao, B., Chen, J., Chen, M., and Li, C. (2008) Mutation of the rice Narrow leaf1 gene, which encodes a novel protein, affects vein patterning and polar auxin transport. *Plant Physiol.* **147**, 1947-1959.

Qi, Y., Wang, S., Shen, C., Zhang, S., Chen, Y., Xu, Y., Liu, Y., Wu, Y. and Jiang, D. (2012) OsARF12, a transcription activator on auxin response gene, regulates root elongation and affects iron accumulation in rice (Oryza sativa). *New Phytol.* **193**, 109-120.

Rea, P.A. (2007) Plant ATP-binding cassette transporters. *Annu. Rev. Plant Biol.* **58**,

347–375.

Romera, F.J., Lucena, C. and Alcántara, E. (2007) Plant hormones influencing iron uptake in plants. In *Iron Nutrition in Plants and Rhizospheric Microorganisms* (Barton, L.L., Abadía, J., Eds). The Netherlands: Springer, 251-278.

Römheld, H. and Marschner, V. (1986) Mobilization of iron in the rhizosphere of different plant species. *Advances in Plant Nutrition* **2**, 155–204.

Sasaki, T., Ezaki, B. and Matsumoto, H. (2002) A gene encoding multidrug resistance (MDR) -like protein is induced by aluminum and inhibitors of calcium flux in wheat. *Plant Cell Physiol.* **43**, 177–185.

Santelia, D., Vincenzetti, V., Azzarello, E., Bovet, L., Fukao, Y., Düchtig, P., Mancuso, S., Martinoia, E. and Geisler, M. (2005) MDR-like ABC transporter AtPGP4 is involved in auxin-mediated lateral root and root hair development. *FEBS Lett.* **579**, 5399–5406.

Schikora, A. and Schmidt, W. (2001) Acclimative changes in root epidermal cell fate in response to Fe and P deficiency: a specific role for auxin? *Protoplasma* **218**, 67–75.

Shen, C., Bai, Y., Wang, S., Zhang, S., Wu, Y., Chen, M., Jiang, D. and Qi, Y. (2010) Expression profile of PIN, AUX/LAX and ABCB auxin transporter gene families in Sorghum bicolor under phytohormone and abiotic stress. *FEBS Lett.* **277**, 2954–2969.

Shen, C.J., Wang, S.K., Zhang, S.N., Xu, Y.X., Qian, Q., Qi, Y.H. and Jiang, D.A. (2013) OsARF16, a transcription factor, is required for auxin and phosphate starvation response in rice (*Oryza sativa* L.). *Plant Cell Environ.* **36**, 607-620.

Shitan, N., Bazin, I, Dan, K., Obata, K., Kigawa, K., Ueda, K., Sato, F., Forestier, C. and Yazaki, K. (2003) Involvement of CjMDR1, a plant multidrug-resistance-type

ATP-binding cassette protein, in alkaloid transport in Coptis japonica. *Proc. Natl. Acad. Sci. USA,* **100**, 751–756.

Sidler, M., Hassa, P., Hasan, S., Ringli, C. and Dudler, R. (1998) Involvement of an ABC transporter in a developmental pathway regulating hypocotyl cell elongation in the light. *Plant Cell*, **10**, 1623–1636.

Teale, W.D., Paponov, I. and Palme, K. (2006) Auxin in action: signalling, transport and the control of plant growth and development. *Nat. Rev. Mol. Cell Biol.* **7**, 847–859.

Terasaka, K., Blakeslee, J.J., Titapiwatanakun, B., Peer, W.A., Bandyopadhyay, A., Makam, S.N., Lee, O.R., Richards, E.L., Murphy, A.S., Sato, F. and Yazaki, K. (2005) ABCB4, an ATP binding cassette P-glycoprotein, catalyzes auxin transport in *Arabidopsis thaliana* roots. *Plant Cell*, **17**, 2922-2939.

Titapiwatanakun, B., Blakeslee, J.J., Bandyopadhyay, A., Yang, H., Mravec, J., Sauer, M., Cheng, Y., Adamec, J., Nagashima, A., Geisler, M., Sakai, T., Friml, J., Peer, W.A. and Murphy, A.S. (2009) ABCB19/ABCB19 stabilises PIN1 in membrane microdomains in Arabidopsis. *Plant J*. **57**, 27-44.

Wang, B., Bailly, A., Zwiewka, M., Henrichs, S., Azzarello, E., Mancuso, S., Maeshima, M., Friml, J., Schulz, A. and Geisler, M. (2013) Arabidopsis TWISTED DWARF1 functionally interacts with auxin exporter ABCB1 on the root plasma membrane. *Plant Cell,* **25**, 202-214.

Wintermans, J.F.G.M. and De Mots, A. (1965) Spectrophotometric characteristics of chlorophylls *a* and *b* and their pheophytins in ethanol. *Biochim. Biophys. Acta* **109,** 448–453.

Woodward, A.W., Bartel, B. (2005) Auxin: regulation, action, and interaction. *Ann. Bot.* **95**, 707–735.

Wu, G., Lewis, D.R. and Spalding, E.P. (2007) Mutations in Arabidopsis multidrug resistance-like ABC transporters separate the roles of acropetal and basipetal auxin transport in lateral root development. *Plant Cell,* **19**, 1826–1837.

Wu, T., Zhang, H.T., Wang, Y., Jia, W.S., Xu, X.F., Zhang X.Z. and Han Z.H. (2012) Induction of root Fe(lll) reductase activity and proton extrusion by iron deficiency is mediated by auxin-based systemic signalling in Malus xiaojinensis. *J. Exp. Bot.* **63**, 859–870.

Yamamoto, M. and Yamamoto, K.T. (1998) Differential effects of 1-naphthaleneacetic acid, indole-3-acetic acid and 2,4-dichlorophenoxyacetic acid on the gravitropic response of roots in an auxin-resistant mutant of arabidopsis, aux1. *Plant Cell Physiol.* **39**, 660-664.

Yang, H. and Murphy, A.S. (2009) Functional expression and characterization of Arabidopsis ABCB, AUX1 and PIN auxin transporters in Schizosaccharomyces pombe. *Plant J.* **59**, 179–191.

Yang, Y., Hammes, U.Z., Taylor, C.G., Schachtman, D.P. and Nielsen, E. (2006) High-affinity auxin transport by the AUX1 influx carrier protein. *Curr. Biol.* **16**, 1123-1127.

Yoshida, S., Forno, D.A., Cock, J.H. and Gomez, K.A. (1976) Routine procedures for growing rice plants in culture solution, Ed 3. International Rice Research Institute, Los Banos, Philippines.

Yu, J. and Wen, C.K. (2013) Arabidopsis aux1[rcr1] mutation

alters AUXIN RESISTANT1 targeting and prevents expression of the auxin reporter DR5:
GUS in the root apex. *J. Exp. Bot.* **64**, 921-933.

Zhang, Y., Su, J., Duan, S., Ao, Y., Dai, J., Liu, J., Wang, P., Li, Y., Liu, B., Feng, D., Wang, J. and Wang, H. (2011) A highly efficient rice green tissue protoplast system for transient gene expression and studying light/chloroplast-related processes. *Plant Methods*, **7**, 30.

Figure 1. Identification of *osabcb14* mutants and complemented lines.

(a) TOS17 insertion sites in *osabcb14-1* and *osabcb14-2*. Black boxes represent the exons, and black lines represent the introns. The inverted triangle marks the insertion site.

(b) PCR analysis of the integration sites of TOS17 in *osabcb14-1* and *osabcb14-2*. The upper bound and the lower bound indicate the *OsABCB14* gene fragment and TOS17 insertion fragment, respectively.

(c) RT-PCR analysis. The upper bands show *OsABCB14* gene expression (30 cycles) and the lower bands show *OsACTIN* gene expression (26 cycles).

(d) qRT-PCR analysis. The relative expression level of *OsABCB14* gene in the mutant lines (*osabcb14-1* and *osabcb14-2*) and the complementation lines (*osabcb14-1*C and *osabcb14-2*C). *OsACTIN* gene was used as an internal control. qRT-PCR experiments was analyzed using three independent biological repeats. * indicates significant difference at P < 0.05 and ** at P < 0.01.

(e)(f) and (g) Phenotype of *osabcb14* mutants and complemented transgenic lines for seven-day seedlings under CK, 2,4-D and IAA treatments. (e) CK. (f) 2,4-D treatment. (g) IAA treatment. Bar = 2 cm.

(h)(i) Shoot length (h) and PR length (i) in *osabcb14* mutants and complemented transgenic lines under various concentrations of 2,4-D treatment.

(j)(k) Shoot length (j) and PR length (k) in *osabcb14* mutants and complemented transgenic lines under various concentrations of IAA treatment.

Figure 2. Expression pattern of *OsABCB14*.

(a) Relative expression level of *OsABCB14* in each tissues of NIP at different growth stage. NIP was cultivated in normal culture solution for three weeks and transferred to field.

(b) The spatial expression of *OsABCB14* in root. Roots of NIP were sampled from the root tips (0 to 1 cm) or basal root zones (1 to 2 cm from the root tip).

(c) to (j) GUS staining in root tip (c), stele (d), leaf blade (e), cross section of leaf sheath (f), node (g), internode (h), root-stem transition region (i) and flower (j). (c)(d) and (f), bar=200µm; (e)(g)(h)(i)(j), bar=400µm.

(k) *OsABCB14* expression of response to various treatments. Seven-day-old seedlings grown in normal culture solution were treated for 3 h with 1 µM 2,4-D, 10 µM IAA, 1 µM NAA, 1 µM 6-BA, 10 µM ABA, 10 µM GA$_3$, 1 mM SA, 1 µM NPA or 10 µM NOA. Total RNA from shoots were analyzed with qRT-PCR.

(l)(m) Expression of *OsABCB14* in 1 µM 2,4-D (l) or 10 µM IAA treatments (m) at indicated time intervals. Seven-day-old seedlings grown in normal culture solution were exposed to 1 µM 2,4-D (l) or 10 µM IAA treatments (m) until shoots were sampled at indicated time intervals. (a) to (m) All qRT-PCR experiments were analyzed using three independent biological repeats. *OsACTIN* gene was used as an internal control.

Figure 3. Subcellular localization of OsABCB14-GFP.

(a) OsABCB14-GFP fusion protein transiently expressed in tobacco. Colocalizaton of OsABCB14-GFP fusion protein with the plasma-membrane marker pm-rb CD3-1008 (Nelson *et al*., 2007), a fusion protein of a red fluorescent protein with a plasma membrane-localized aquaporin. Left to right: green fluorescence of OsABCB14-GFP, red fluorescence of pm-rb CD3-1008, bright-field, merged microscope images. Bar=20 µm.

(b) Transient expression of the OsABCB14-GFP fusion protein in onion epidermis cells before plasmolysis. Left to right: green fluorescence of OsABCB14-GFP, bright-field, merged microscope images. Bar=50 µm.

(c) Transient expression of OsABCB14-GFP fusion protein in onion epidermis cells after plasmolysis. Left to right: green fluorescence of OsABCB14-GFP, bright-field, merged microscope images. Bar=50 µm.

Figure 4. Auxin concentration in *osabcb14* mutants.

(a) Free IAA concentration in shoot of seven-day seedlings.

(b) Free IAA concentration in PR of seven-day seedlings.

(c) *DR5:GUS* staining in leaf sheath cross section of five-day seedlings. Bar=200 µm.

(d) *DR5:GUS* staining in PR of five-day seedlings. Bar=200 µm. Experiments in (a)(b)(c) and (d) were analyzed using five independent biological repeats.

(e)(f) qRT-PCR analysis for auxin-responsive genes in shoots (e) and roots (f) of NIP and *osabcb14* mutants of seven-day seedlings. qRT-PCR experiments were analyzed using three independent biological repeats. *OsACTIN* gene was used as an internal control.

Figure 5. **Auxin transport activity in yeast and *osabcb14* mutants**

(a) Retention of IAA and of the diffusion control, benzoic acid (BA), in vector control (VC) or OsABCB14 yeast cells (strain JK93da).

(b) IAA and NAA import into NIP or *osabcb14-1* and *osabcb14-2* protoplasts. Values are

mean activities ± SEs of four individual measurements (n = 4).

(c) IAA and NAA export from NIP or *osabcb14-1* and *osabcb14-2* protoplasts. Values are mean activities ± SEs of four individual measurements (n = 4).

(d) Acropetal ^{3}H-IAA transport from the root tip (1cm) of three-day seedlings.

(e) Basipetal ^{3}H-IAA transport from the root tip (1cm) of three-day seedlings.

Experiments were analyzed using four independent biological repeats for (a)(b)(c) and five for (d)(e). * indicates significant difference at $P < 0.05$ and ** at $P < 0.01$.

Figure 6. Fe concentration and phenotype in *osabcb14* mutants.

(a) Fe concentration of seeds, shoots and roots. Left to right: seeds, shoots for fourteen-day seedlings grown in normal nutrition, roots for fourteen-day seedlings grown in normal nutrition.

(b) Phenotype of *osabcb14* mutants under CK and -Fe treatments. Bar = 5 cm.

(c)(d) Shoot length (c) and PR length (d) of fourteen-day seedlings under CK and -Fe treatments.
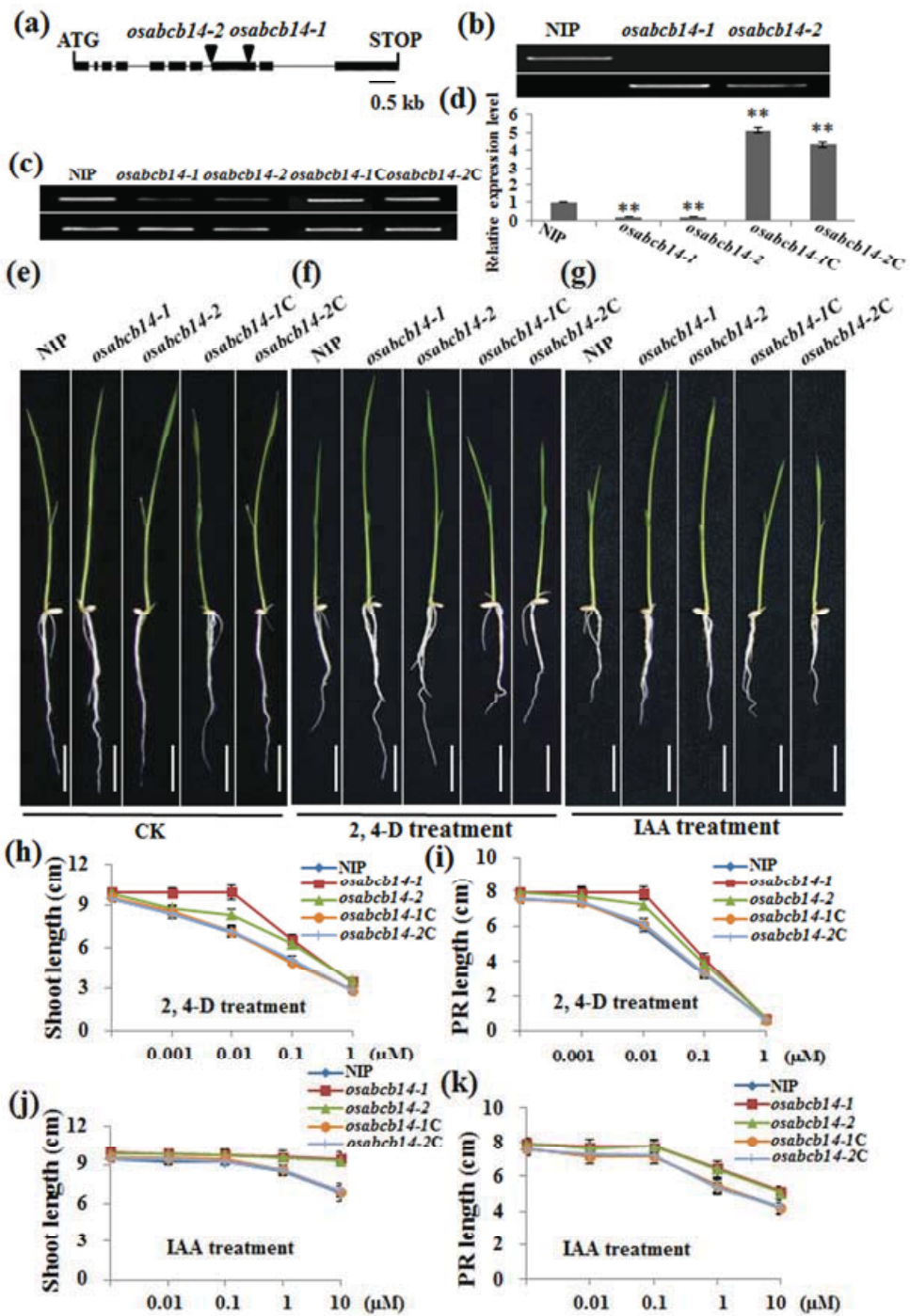
(e) Chlorophyll concentration of fourteen-day seedlings under CK and -Fe treatments.
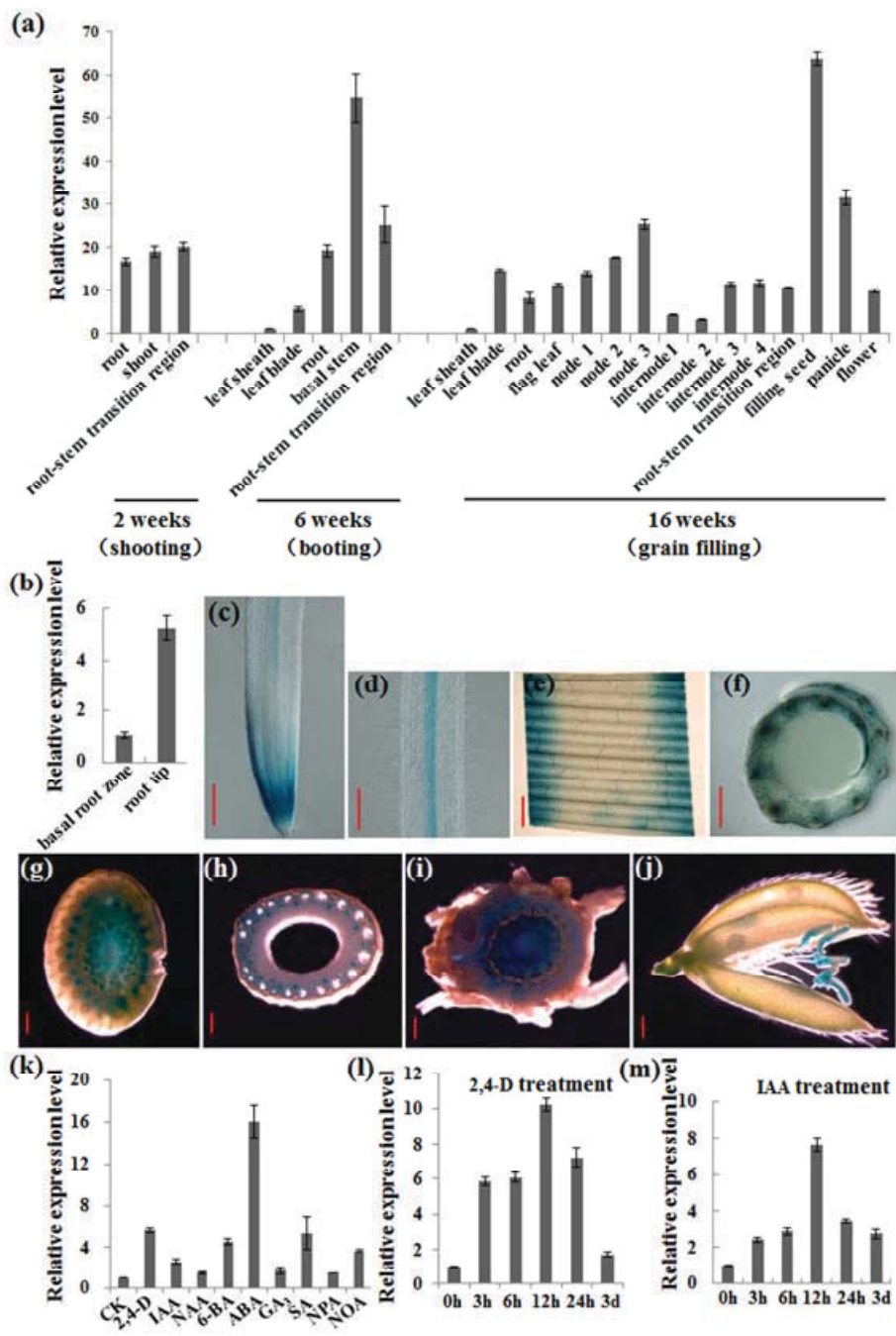
(f)(g) Fe concentration of shoot (f) and root (g) for fourteen-day seedlings under -Fe treatments (g). (a) to (g) All experiments were analyzed using five independent biological repeats. * indicates significant difference at P < 0.05 and ** at P < 0.01. CK: normal culture solution.

Figure 7. Relative expression of genes related to Fe uptake and transport in shoots of NIP and *osabcb14* mutants.

(a) qRT-PCR analysis for genes related to Fe response in shoots of NIP and *osabcb14* mutants.

(b) qRT-PCR analysis for genes related to Fe response in shoots of NIP and *osabcb14* mutants under CK and –Fe. (a)(b) All qRT-PCR experiments were analyzed using three independent biological repeats. *OsACTIN* gene was used as an internal control. CK: normal culture solution. * indicates significant difference at P < 0.05 and ** at P < 0.01.

(a) ATG *osabcb14-2 osabcb14-1* STOP
0.5 kb

(b) NIP *osabcb14-1 osabcb14-2*

(c) NIP *osabcb14-1 osabcb14-2 osabcb14-1*C*osabcb14-2*C

(d) Relative expression level

(e) NIP *osabcb14-1 osabcb14-2 osabcb14-1*C *osabcb14-2*C
(f) NIP *osabcb14-1 osabcb14-2 osabcb14-1*C *osabcb14-2*C
(g) NIP *osabcb14-1 osabcb14-2 osabcb14-1*C *osabcb14-2*C

CK   2, 4-D treatment   IAA treatment

(h) Shoot length (cm) — 2, 4-D treatment
NIP
osabcb14-1
osabcb14-2
*osabcb14-1*C
*osabcb14-2*C
0.001 0.01 0.1 1 (μM)

(i) PR length (cm) — 2, 4-D treatment
NIP
osabcb14-1
osabcb14-2
*osabcb14-1*C
*osabcb14-2*C
0.001 0.01 0.1 1 (μM)

(j) Shoot length (cm) — IAA treatment
NIP
osabcb14-1
osabcb14-2
*osabcb14-1*C
*osabcb14-2*C
0.01 0.1 1 10 (μM)

(k) PR length (cm) — IAA treatment
NIP
osabcb14-1
osabcb14-2
*osabcb14-1*C
*osabcb14-2*C
0.01 0.1 1 10 (μM)

36